# From powder to cloth: Facile fabrication of dense MOF-76(Tb) coating onto natural silk fiber for feasible detection of copper ions



doi: 10.1016/j.cej.2018.05.144

# From powder to cloth: facile fabrication of dense MOF-76(Tb) coating onto natural silk fiber for feasible detection of copper ions

Jie Li[a,b,d], Xiao Yuan[b,d], Yi-nan Wu[b,d,*], Xiaoliang Ma[b,d], Fengting Li[b,c,d], Bingru Zhang[b,c,d], Ying Wang[b,c,d,*], Zhongfang Lei[a,*], Zhenya Zhang[a]

[a] Graduate School of Life and Environmental Sciences, University of Tsukuba, 1-1-1 Tennodai, Tsukuba, Ibaraki 305-8572, Japan

[b] College of Environmental Science & Engineering, State Key Laboratory of Pollution Control and Resource Reuse Study, Tongji University, 1239 Siping Road, Shanghai 200092, China

[c] UNEP-Tongji Institute of Environment for Sustainable Development, Tongji University, Shanghai 200092, China

[d] Shanghai Institute of Pollution Control and Ecological Security, Shanghai 200092, P.R. China

*Corresponding authors.

Email addresses: 51n@tongji.edu.cn (Y. Wu), yingwang@tongji.edu.cn (Y. Wang), lei.zhongfang.gu@u.tsukuba.ac.jp (Z. Lei)

**Abstract**

The deposition of powdered MOFs material onto other substrates is essential to avoid inconvenience during its practical applications. In this work, domestic silk fiber was utilized as the skeleton, for successful coating of dense luminescent MOF-76(Tb). Its surface functionality which consist of abundance of intrinsic carboxylic groups, smooth surface structure, and 80% of tensile strength were maintained after being immersed in different thermal solvents (water, ethanol, DMF @ 80 °C) for 24 h, revealing good solvent and thermal resistance. By using hydrothermal, microwave assisted, and layer-by-layer methods, different crystal morphologies (pillar-like, sedimentary-rock-like, and needle-like morphology) and varying degrees of surface coverage rate were obtained, as a result of different levels of anchoring promotion and crystal controlling effect. The MOFs coating can be confirmed by its XRD pattern and fluorescent property. More importantly, the quenching effect of the composite in a condition of $Cu^{2+}$ was first reported with high selectivity, sensitivity (i.e. a linear detection concentration range of $10^{-3}$–$10^{-5}$ M with a low detection limit up to 0.5 mg/L, $K_{SV}$ of 1192 $M^{-1}$ at 293 K), and rapid response time (5 min), making the composite a good candidate for colorimetric and fluorescent detection of aquatic $Cu^{2+}$. The quenching mechanism is proposed to associate with the interaction between $Cu^{2+}$ and benzene-tricarboxylate (BTC) ligand, which resulted in the decrease of energy transfer efficiency. The selectivity over other common cations depends on the unsaturated electron configuration and the smaller ionic radius of $Cu^{2+}$.

**Keywords:** MOF-76(Tb); natural silk fiber; dense coating; $Cu^{2+}$ detection

## 1. Introduction

Metal–organic frameworks (MOFs), in which metal ions act as coordination centers and link together with organic ligands through self-assembly processes [1], have been extensively studied for various applications in the past two decades [2, 3]. Recently, lanthanide-based MOFs, one type of MOFs materials possessing unique luminescence properties such as high luminescence quantum yield, long-lived emission, large Stokes shifts, and characteristically sharp line emissions [4-6], have attracted considerable attention due to their marketable potential for chemical sensing [7-9]. In theory, the combination of luminescence and accessible porosity within MOFs confers these materials with detection capacity through the luminescence intensity change [8], thus making them become promising candidates in chemical sensing. Among the various kinds of lanthanide-based MOFs materials that have been developed, $Tb(BTC)(H_2O)_{1.5}\cdot(DMF)$ labeled as MOF-76(Tb), outperforms other materials due to its simple work-up procedure, mild reaction conditions, high yield, and high purity [10]. Furthermore, owing to its luminescent properties, MOF-76(Tb) has been explored for detection of $F^-$ [11], U(VI) [12], aromatic pollutants [13], and small organic molecules [14, 15], etc., thus, exhibiting promising detection potential.

Although the usage of luminescent MOFs for sensing has been attempted, the inherent characteristics of powdered materials are considered to restrict their further application in real practice. Especially, fluorescent sensing in the homogeneous phase is not suitable for enrichment and removal of target species [16-18]. To date, MOFs as components of a commercial functional sensing device, have not been reported [19].

When being used as sensors, catalytic coatings, filters, or other devices, the deposition of MOFs onto solid substrate is essential and is recognized as one of the most critical issues [20-23]. Some trials have been done to prepare a luminescent MOFs material-coated magnetic sphere, for easy recycling of the sensor material [7]. Meanwhile, considerable work have been done on deposition of thin MOFs films onto different substrates, such as polyester fabric [24], pulp fibers [25], and porous alumina [20], yielding suitable materials for sensors. For all these substrate materials, however, their functionalization through atomic layer deposition (ALD) coating or formation of self-assembled monolayers (SAMs) is required as pretreatment [26], thereby increasing the complexity and cost of the whole process.

The silkworm fibroin (domestic silk), mainly consisting of glycine, alanine and sericine [27], is a fibrous protein and has been universally established as one kind of textile fibers due to its unique handle and mechanical properties. The repeated -Gly-Ala-Gly-Ala-Gly-Ser- motif in fibroin contributes a lot to the strength and stiffness of the silk, through the formation of high volume fraction of $\beta$-sheet microcrystallites [28]. In addition, theoretically, no functionalization or pretreatment is needed when fibroin fiber is used as the substrate because the reactive carboxylic groups are abundant on its surface, which are essential for the deposition of the initial MOFs layer [9, 29, 30]. Whereas further verifications for its solvent resistance and thermal stability are necessary because these properties generally dictate the possible utilization of composite in practice. Given that the procedure for deposition usually determines the quality of the coated MOFs layer, various synthesis methods can be applied for the

deposition of MOF material onto the silk fibroin fiber [24, 31], which may offer different coating efficiency and performance.

Copper (II) ($Cu^{2+}$) is a typical micronutrient element. Excessive exposure to copper should be avoided due to its negative impact on human health [32]. However, copper pollution in waterbodies has frequently occurred in the past decades because of uncontrolled anthropogenic activities [33]. Thus, highly sensitive and selective methods for fast and reliable sensing of $Cu^{2+}$ are crucial for water environment protection and human health safety. Among the various methods developed for the detection of trace copper in aquatic environment, the fluorescence-based method shows considerable application potential because of its simplicity, quick response time for on-site analysis, and cost-effective instrumentation, which can be easily assembled in small and low-power packages [7, 16, 34, 35].

In this work, natural fibroin fiber was selected as the substrate for the deposition of MOF-76(Tb). The solvent resistance and the surface property of the silk substrate were investigated. The coating efficiency of three methods, namely hydrothermal (HT), microwave assisted (MWA), and layer-by-layer (LBL) methods were compared with related factors being analyzed. In addition, this work for the first time, demonstrated the extended usage of the MOF-76(Tb)@silk fiber composite for fluorescent/colorimetric sensing of copper ion ($Cu^{2+}$).

## 2. Experimental section

### *2.1. Materials*

All materials and chemicals were of reagent grade and used without further

purification. Terbium nitrate hexahydrate and 1,3,5-benzenetricarboxylic acid were purchased from Alfa Aesar. Metal nitrates (potassium nitrate, sodium nitrate, aluminum nitrate, iron nitrate, calcium nitrate, lead nitrate, nickel nitrate, zinc nitrate, cadmium nitrate, and copper nitrate) and organic solvents (ethanol, methanol, *N*,*N*-dimethylformamide (DMF), and *n*-hexane) were supplied by Sinoreagent. Silkworm cocoons were purchased from a local silk farm in China. Deionized water was used throughout this work.

Silk fibroin fiber was prepared from silkworm cocoon through a degumming procedure, so as to remove the coat of sericin proteins [36-38]. The degumming treatment was processed according to a previous study [28]. The procedure is as follows: the silkworm cocoons were first rinsed in water to get rid of the surface contaminants and were then cut into small fragments with an average size of 1 $cm^2$. Then, the silk fiber was degummed in boiling water for 30 min. In order to ensure maximum sericin removal, the fine fibers were further degummed in a 0.1M $Na_2HCO_3$ solution at 90–100 °C for 30 min and washed with deionized water for 3 times. Finally, the sample was dried at 100 °C for 6 h before testing and further usage.

*2.2. Material characterization*

Fourier transform infrared (FTIR) spectra of the silk fiber, before and after immersion were obtained using a FTIR spectrophotometer (Nicolet 5700, USA). Scanning electron microscopy (SEM) images were observed using a field emission scanning electron microscope (FESEM) on a JEOL JSM-5400 system, at an accelerating voltage of 15 kV. The mechanical property of the silk fiber was measured by an electronic universal

testing machine (UTM 2502, China). The crystal structure of the coated material was obtained by X-ray powder diffractometer (XRD, D8 Advance, Germany), and the data was processed in a continuous scanning mode within the range of 3°–50°, at a step width of 0.02° and scanning speed of 5°/min.

*2.3. Preparation of MOF-coated silk fibers*

Three synthesis methods, i.e. HT, MWA and LBL, were applied for MOF-coated silk fiber preparation and then compared in this study.

In the typical HT method, 0.120 g of $Tb(NO_3)_3 \cdot 6H_2O$ (0.28 mmol) and 0.020 g of $H_3BTC$ (0.10 mmol) were dissolved in the mixture of DMF (4.0 mL), ethanol (4.0 mL), and $H_2O$ (3.2 mL). Then the reaction mixture was stirred for 1 h and later poured into a solvothermal vessel containing 70 mg of silk fiber. The vessel was sealed and heated to 80 ˚C at a rate of 2 ˚C/min for 24 h to obtain white precipitates. The obtained materials were washed with ethanol and dried at 80 ˚C in vacuum for further use [39].

In the typical MWA synthesis [13], the same mixture solution used in the HT method was transferred into a microwave vessel containing 70 mg of silk fiber. Then the vessel was sealed and heated to 80 ˚C at a heating rate of 2 ˚C /min for a certain amount of time. The obtained white precipitates were washed thrice with ethanol and then dried in vacuum for further use.

In the typical preparation by the LBL method [40], a mixture of $Tb(NO_3)_3 \cdot 6H_2O$ (0.120 g, 0.28 mmol), DMF (4.0 mL), ethanol (4.0 mL), and $H_2O$ (3.2 mL) was termed as the precursor solution A. The precursor solution B was the mixture of $H_3BTC$ (0.120 g, 0.28 mmol), DMF (4.0 mL), ethanol (4.0 mL), and $H_2O$ (3.2 mL). The weighed silk

fibers (70 mg) were dipped in solutions A and B for 4 h, alternatively. After each dipping, the silk fiber was rinsed in ethanol to remove the unreacted precursor. After a few preparation cycles, the samples were dried in vacuum for further use.

*2.4. Luminescent sensing procedures*

All the luminescence sensing measurements were performed at room temperature by a Horiba FluoroMax-4 spectrofluorophotometer with the range of 450–650 nm having a fixed excitation wavelength of 303 nm. The luminescence intensity was evaluated by the intensity of the strongest emission ($^5D_4 \rightarrow {}^7F_5$ transition) at 548 nm [41]. The quenching effect was determined by the intensity variation of the MOF-76(Tb)@silk fiber composite before and after the addition of analyte solution.

## 3. Results and discussion

*3.1. Surface properties of silk fiber and its solvent resistance*

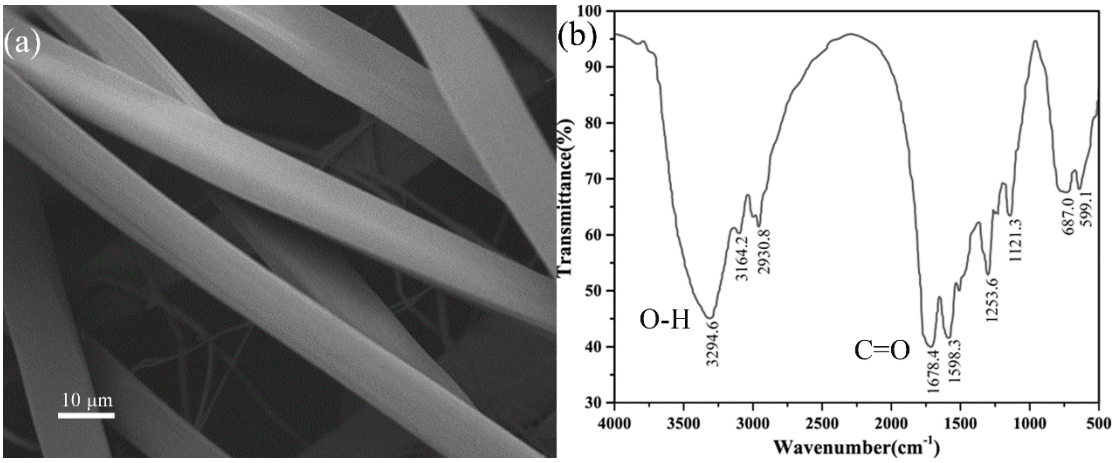


Fig. 1 SEM image (a) and FTIR spectra (b) of the natural silk fibers used in this work.

The SEM image (Fig. 1a) reveals the flattened shape of the pristine silk fiber at a high magnification, the smooth surface of which, in theory, makes it a good fit for coating MOFs material with low roughness [24]. In the IR spectra (Fig. 1b), the broad

peak at 3294.6 $cm^{-1}$ (O–H stretching) and the intensive peak at 1678.4 $cm^{-1}$ (C=O stretching) were ascribed to the stretching vibration of surface carboxylic groups formed from the polymerization of typical amino acids like glycine and alanine [42-44]. The abundant carboxylate linkers on the surface of silk fiber suggest its great potential for coating MOFs material, as functionalization of the substrate surface is essential for the formation of MOFs coating [24, 31].

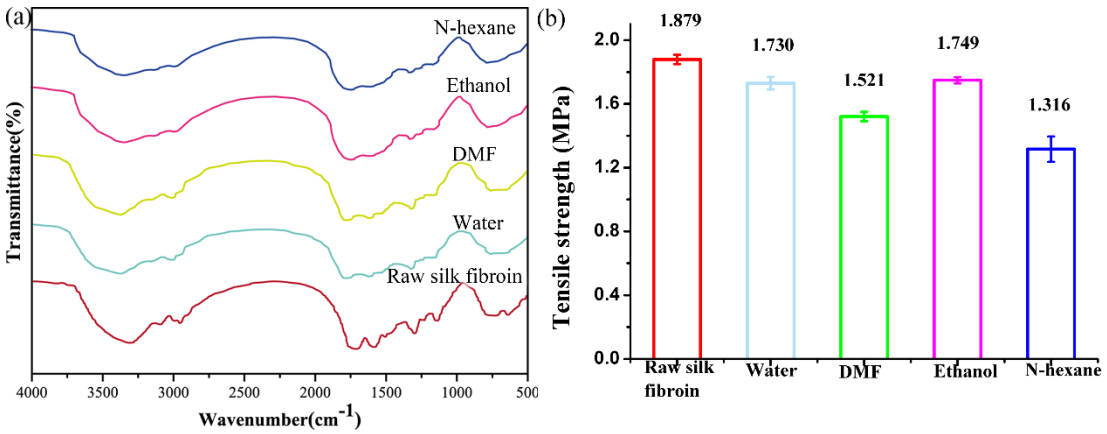


Fig. 2 FTIR spectra (a) and comparison in tensile strength (b) of silk fiber before and after immersion in various solvents at 80 °C for 24 h.

To explore the thermal stability and solvent endurance of the silk fiber, the surface and mechanical properties were compared between the raw material and those after being immersed into the commonly used solvents (water, DMF, ethanol, and *n*-hexane) at 80°C (the synthesis temperature for MOF-76(Tb)). As shown in Fig. 2a, the primary peaks matched well with the raw material, indicating that the main surface functional groups could be maintained after immersion into the tested solvents (polar or nonpolar, organic and inorganic solutions) for 24 h. In addition, each fiber was well proportioned, with a smooth surface and devoid of any apparent deformation, fracture, fold, or

swelling (as shown in the Supplementary Materials, Fig. S1), thereby maintaining the structural properties of the raw silk fiber. In terms of mechanical property, although the tensile strength showed some slight decrease after immersion in the above mentioned solvents (Fig. 2b), the residual tensile strength (1.730 MPa, 1.749MPa, and 1.521MPa in water, methanol, and DMF, respectively) was sufficient for further coating operation and application of the composite material in real practice.

*3.2. Verification of the immobilized MOF-76 via different synthesis methods*

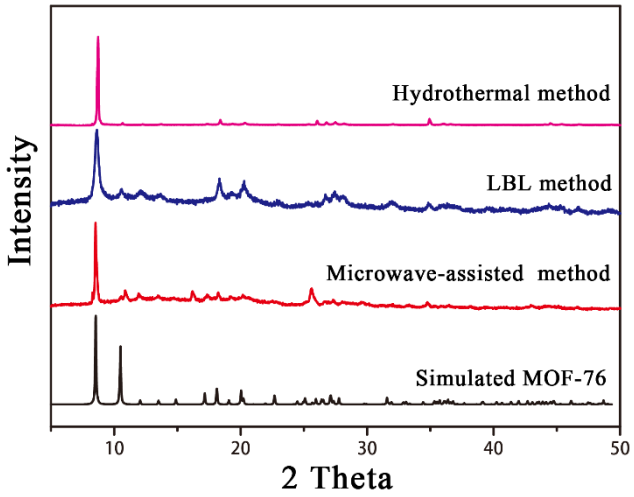


Fig. 3 XRD patterns of the simulated MOF-76(Tb) and MOF-76(Tb)@silk fiber composite prepared with three different approaches, i.e. hydrothermal (HT), layer-by-layer (LBL) and microwave assisted (MWA) methods.

The deposition of MOF-76(Tb) onto the silk fiber was confirmed by XRD patterns of the composite. As shown in Fig. 3, the XRD patterns of the composite material synthesized using three different methods (HT, MWA, and LBL) were identical with that of simulated MOF-76(Tb) pattern, suggesting the successful deposition of MOFs material onto the silk fiber surface [11, 12, 45]. The major diffraction peaks associated

with MOF-76(Tb) at 11 and 8 degrees were observed in all MOF-76(Tb) coated silk fiber samples [11, 14]. The weakened diffraction peak at 11 degrees was resulted from the combination of simulated MOF-76(Tb) spectrum with the silk fiber pattern. The additional broad diffraction peaks observed between 10 and 30 degrees were associated with the characteristic amorphous diffraction peaks of silk fiber [44].

To ensure the full activation of the MOFs coating and bulk MOFs powder, surface area analysis was performed in dynamic vacuum at 120 °C, which is the heat resistance temperature of the natural silk fiber. However, the surface area value was not measurable, indicating that the pores of the material were not accessible to $N_2$. This phenomenon is consistent with the previous statements that MOF-76(Tb) does not allow $N_2$ molecules to enter the pores. It becomes accessible only when the activation temperature is higher than 250 °C [10, 46, 47]. One notable phenomenon is that, after immobilization onto the silk fiber, the reported fluorescence enhancement effect of MOF-76(Tb) was maintained in the case of fluorine ion (Fig. S3), revealing no adverse effect of the deposition process on the fluorescent property and the guest molecule diffusion in the channels of MOF-76(Tb). Thus, the deposition of MOF-76(Tb) with the three different methods was successfully achieved with very limited impact on structural strength, surface area or fluorescence property.

### *3.3. Pillar-like morphology and poor surface coating of MOF-76 via hydrothermal deposition*

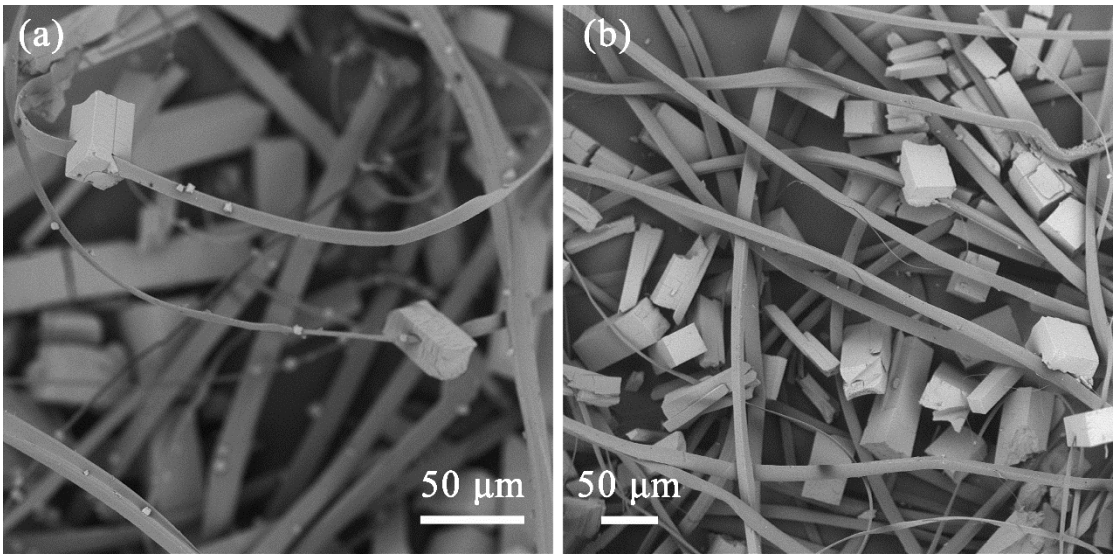


Fig. 4 SEM images of the MOF-76(Tb)@silk fiber composite prepared by the hydrothermal (HT) method: (a) the immobilized crystals perforated by silk fiber; and (b) the detached crystals entrapped by fiber net.

With the HT method, the immobilized crystals revealed an overall morphology of a cubic column (Fig. 4a), which is characteristic of MOF-76(Tb) but about half of the length (40–50 μm) and consequently, half of the weight of conventional MOF-76(Tb) crystals (120 μm, as shown in Fig. S2) [13]. Notably, these crystals were perforated by silk fiber, indicating a process of gradual crystal growth on the fiber surface instead of adhering or attaching of the formed crystal to the fiber. According to the theory of self-assembled monolayers (SAMs) [20, 31], the silk fiber was supposed to anchor the $Tb^{3+}$ ions at first and then proceeded with the crystal growth through self-assembly process subsequently.

Despite the fact that the fiber surface is rich in functional groups which are conducive to anchoring or coordinating with metal ions and then the formation of MOFs coatings, very few crystals were retained, while a large amount of the normal sized crystals

dropped and were entrapped by the fiber net (Fig. 4b). Two factors were proposed that brought about this poor coating efficiency. On one hand, inadequate anchoring of $Tb^{3+}$ resulted in limited amount of nucleation sites for the subsequent crystal growth. On the other hand, the formed crystals were detached because of gravity effect. It can be concluded that only those MOFs crystals, having sufficient bonding force (enough nucleation sites) with the silk fiber and limited crystal size (weight), can work against gravity and remain on the surface. In summary, regarding the HT method, low surface coverage and loading rate was obtained, most probably due to the insufficient anchoring of metal precursors and the high detachment rate of normal sized crystals.

### *3.4. Sedimentary-rock-like morphology and improved coating of MOF-76(Tb) via microwave assisted deposition*

Under the conditions of the MWA method, which involved soaking at a temperature of 80 ˚C (at a heating rate of 2 ˚C/min) for 4 h, a uniform sedimentary-rock-like crystal coverage was obtained (Fig. 5a). The crystal size (with a dimension of approximately 10 μm in length and 5 μm in width and thickness) implies an even lighter weight than the pillar-like crystals, agreeing with the previously reported size reduction effect by using microwave or ultrasound method [48, 49]. In addition, the irregular shape of the crystals revealed that the process was performed by successively depositing the crystal flakes under continuous microwave impact. The enhanced microwave disturbance avoided the complete crystal growth, as that accomplished in a static environment, and instead, gave birth to a gradual deposition of crystal flakes. During the self-assembly processes, interactions between the organic and metal precursors created friction

between flakes, and between flakes and the fiber, which can compensate for gravity and avoid crystal detaching. Notably, an interesting phenomenon occurred, the crystals prepared with the same method but without silk fiber as substrate retained the conventional pillar-like shape. This can be explained by the isotropy of the synthesis environment. That is, the microwave disturbance effect was minimized in a homogeneous environment.

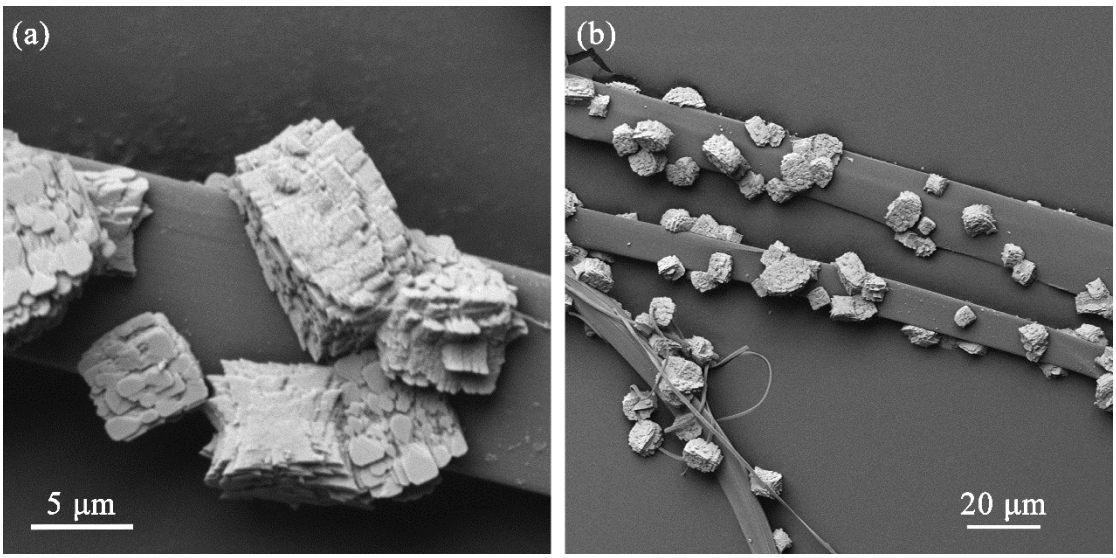


Fig. 5 SEM images of the MOF-76(Tb)@silk fiber composite prepared by the microwave assisted (MWA) method: (a) the morphology of the immobilized crystals; and (b) the surface coverage of MOF-76(Tb) coating onto the silk fiber.

In addition to the conversion of crystal morphology, an obvious improvement of crystal coverage was realized (Fig. 5b), revealing an enhanced process of anchoring $Tb^{3+}$ to form the surface nucleation sites [24]. The higher anchoring efficiency is attributed to the enhanced microwave disturbance which promotes sufficient contact between the fiber and metal ions. To conclude, with the help of microwave disturbance, both increased amount of nucleation sites and limited crystal size/weight were achieved

simultaneously, resulting in improved surface coverage and loading rate of MOF-76(Tb).

*3.5. Needle-like morphology and dense coating of MOF-76(Tb) via layer-by-layer deposition*

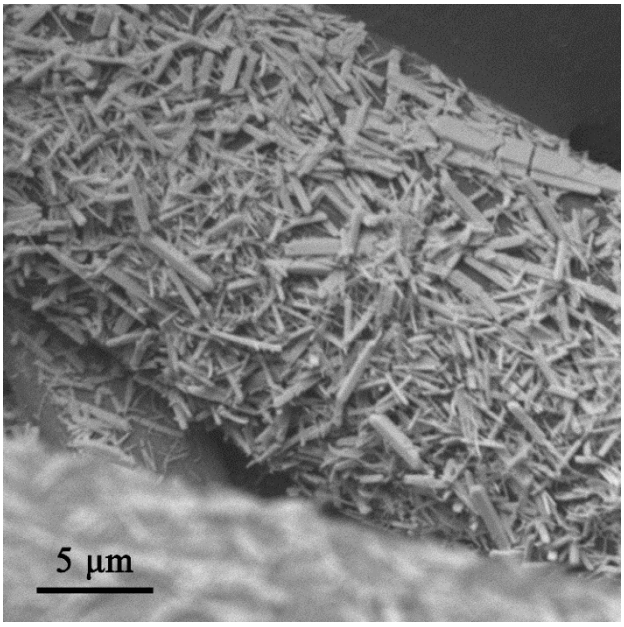


Fig. 6 SEM image of the MOF-76(Tb)@silk fiber composite prepared by the layer-by-layer (LBL) method.

For the composite prepared by the LBL method, the crystal surfaces of the coated MOF-76(Tb) were clearly distinguished (Fig. 6), reflecting an overall uniform needle-like morphology and a further controlled crystal size (5–10 μm in length and <1 μm in width). In the above trials, with the HT and MWA method, the MOF-silk composite still had distinct fiber regions that remained exposed after immobilization of MOF-76. In contrast, by using the LBL method, the silk fibers could be completely coated with the MOF-76 crystal material. The deposition process was monitored by SEM imaging (Fig. 7), which reflected obvious surface coverage improvement after each growth cycle.

More importantly, even after being washed several times with ethanol, the coated MOF-76 crystals still remained on the fiber surface, revealing excellent binding force between the crystal and the silk fiber.

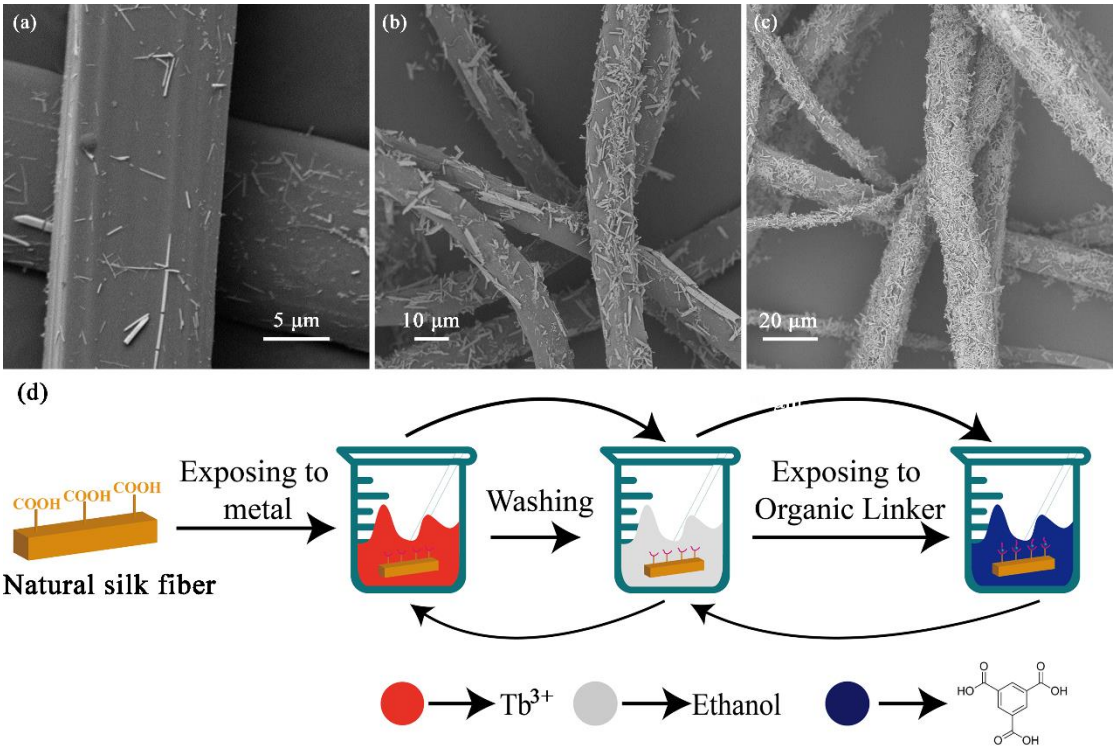


Fig. 7 SEM images of the MOF-76(Tb) coated silk fibers prepared by the LBL method after the first cycle (a), third cycle (b), and fifth cycle (c), and (d) the schematic of the layer-by-layer (LBL) assembly technique used for the deposition.

Besides the limited overall size of the coated MOF-76(Tb) and its needle-like shape, it was found that the crystal size of MOF-76(Tb) formed in the outer layer increased gradually (Figs. 7a-7c). During each synthesis cycle, a certain amount of the precursor was consumed to form the inner layer of MOF-76(Tb) coating and increase the surface coverage ratio; meanwhile, the rest formed the outer layer coating. With more accessible binding sites supplied by the previously formed inner coating layer, the

limiting step of metal ion anchoring for the outer layer formation could be skipped. Accordingly, the crystal size increased rapidly because they could overcome the gravity effect.

For the LBL method, the dramatic increase in surface coverage is most likely associated with the variation in the synthesis procedure. The repeated immersion and cycling in the separated MOF precursor solutions restricted the continuous crystal growth and instead, promoted the anchoring of metal ions through the surface carboxylic groups (Fig. 7d) [44]. To conclude, such a high loading efficiency through the LBL method is mainly attributable to the following aspects: (1) the promotion of anchoring metal ions accelerated the full coverage of inner coating layers; (2) the strictly controlled crystal growth prevented the detachment of formed crystals caused by overweight effect; and (3) the formation of multi-coating layers further increased the loading rate. All these aspects were conducive to the dense coating of MOFs layer onto the surface of silk fibers. Compared with the previously reported works using sodium acetate as the capping reagent, the variation in the synthesis procedure is more efficient in the formation of more nucleation sites and in controlling the crystal size [13, 50, 51].

Table 1. Contribution of related factors to MOF-76(Tb) coating onto silk fiber

| | HT method | MWA method | LBL method |
|---|---|---|---|
| Metal anchoring promotion | × | √ | √ √ |
| Crystal growth control | × | √ | √ √ |
| Coating efficiency | Low | Medium | High |

Note: × - little effect, √ - good effect, √ √ - better effect

Taken together, for the immobilization of MOFs onto silk fiber, both the anchoring of $Tb^{3+}$ and the crystal growth play an important role in the preparation process. The former process forms the nucleation sites for surface crystal growth, and the latter determines the detachment ratio of the formed crystals. Among the HT, MW, and LBL methods, varying degrees of anchoring promotion and crystal controlling were achieved, resulting in different coating and loading rates of MOF-76(Tb) onto the natural silk fiber (Table 1).

*3.6. MOF-76@silk fiber composite as a potential chemical sensor for colorimetric and fluorescent detection of aquatic $Cu^{2+}$*


Fig. 8 Fluorescence images of the MOF-76(Tb)@silk fiber composite after immersion in equal volumes of solutions containing different metal ions (0.5 mM of $M(NO_3)_x$, M = $K^+$, $Na^+$, $Al^{3+}$, $Fe^{3+}$, $Ca^{2+}$, $Pb^{2+}$, $Ni^{2+}$, $Cd^{2+}$, and $Cu^{2+}$).

An obvious quenching effect of the composite was detected after immersion in 0.5 mM of copper-containing solutions (as shown in Fig. 8). The disappearance of typical green fluorescence and a clear change in color from green to grey could be used to make a qualitative judgment in the existence of copper. The intensity of the composite at 548 nm was influenced by cations, especially in the case of $Cu^{2+}$, showing an obvious selectivity for copper ions (Fig. 9a). Thus, the silk fibroin-based composite can be proposed for colorimetric sensing of $Cu^{2+}$ in aqueous solution.

The recognition of $Cu^{2+}$ might be related with the interaction between $Cu^{2+}$ and the

carboxylate oxygen sites on the pore surface of MOF-76(Tb). The interaction between the $Cu^{2+}$ and the benzene-tricarboxylate (BTC) ligands reduced the energy transfer efficiency from BTC to the $Tb^{3+}$ within MOF-76(Tb), thus decreasing the luminescent intensity [52]. Alkali earth cations like $Na^{+}$ and $K^{+}$, with saturated electron configuration, almost have no effect on the luminescent intensity [53]. Other divalent and trivalent cations including $Ca^{2+}$, $Pb^{2+}$, $Zn^{2+}$, $Cd^{2+}$, and $Al^{3+}$ with a close-shell electron configuration, display a light quenching effect due to the weak interaction between Lewis basic sites and metal ions [53, 54]. Although being similar to $Cu^{2+}$, with an unsaturated electron configuration, $Ni^{2+}$ does not show obvious quenching effect, probably due to the limitation of its ionic radius. In summary, the unique quenching effect for $Cu^{2+}$ possibly resulted from the unsaturated electron configuration and the smaller ionic radius [55].

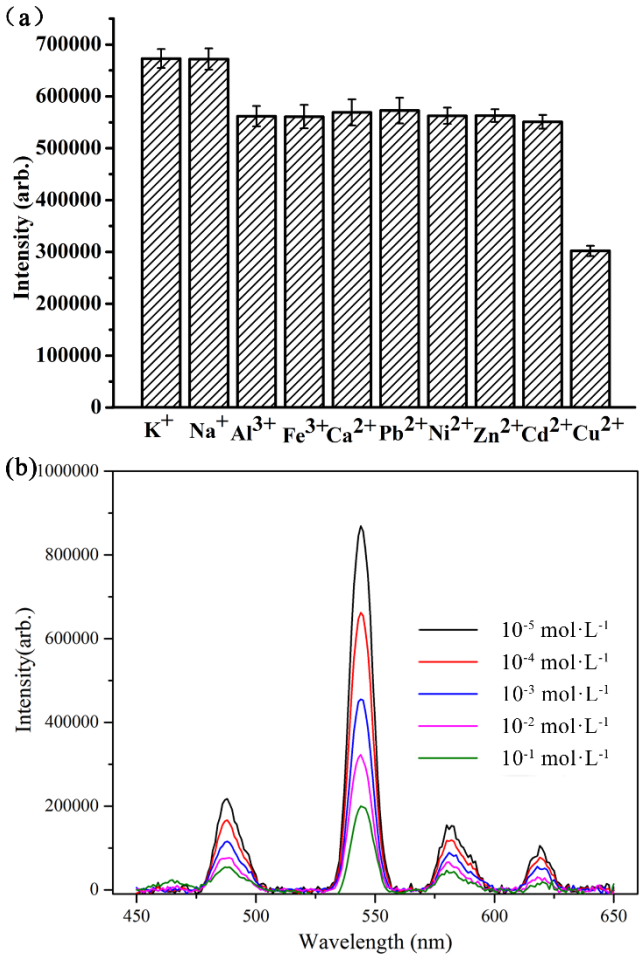


Fig. 9 (a) Luminescence intensity of the MOF-76(Tb)@silk fiber in 0.5 mM of various cation-containing solutions (at 546 nm), and (b) PL spectra of the silk fibroin net in aqueous solutions containing different $Cu^{2+}$ concentrations.

Initially, the kinetic characteristic for $Cu^{2+}$ detection using the MOF-76@silk fiber composite was tested in this study. Upon the addition of $Cu^{2+}$, the fluorescence emission decayed within the initial 5 min and maintained equilibrium subsequently. Therefore, for the following experiments, a reaction time of 5 min was set to ensure the fluorescence equilibrium before measurement. This rapid response is probably brought about by the facile diffusion of $Cu^{2+}$ ions across the porous structure of MOF-76(Tb).

Sensitivity is another important factor for evaluating on the performance of the

composite material and in the determination on the trace amount of $Cu^{2+}$. The silk composites were immersed in solutions with gradually increasing $Cu^{2+}$ concentration to further probe its luminescence response property. As shown in Fig. 9b, the luminescence intensity of the fiber composite was highly sensitive to the $Cu^{2+}$ concentration, and the intensity at 548 nm was almost completely quenched at a concentration of $1\times10^{-2}$ M of $Cu^{2+}$. The relative luminescence intensity at 548 nm versus the concentration of $Cu^{2+}$ plot showed a decreasing trend, which could be well fitted to a first-order exponential equation ($R^2$ of 0.996, Fig. S4), indicating a diffusion-controlled process for its quenching behavior [52, 55]. In addition, a linear fit of $I_0/I$ ratio to copper concentration could be established (Fig. S5), reflecting the linear dependence of luminescent quenching on the concentration of $Cu^{2+}$ (i.e., the $I_0/I$ ratio is virtually linearly correlated with the copper concentration within the range of $1\times10^{-3}$–$1\times10^{-5}$ M). Even at a low $Cu^{2+}$ concentration of 0.5 mg/L, the decrease in luminescent intensity was still detectable. In conclusion, the high selectivity and sensitivity of MOF-76@silk fiber composite makes it a suitable candidate in the application of colorimetric and fluorescent detection of $Cu^{2+}$.

The quenching effect can also be approximately illustrated by the Stern–Volmer equation ($I_0/I = 1 + K_{SV}$ [M]). As for the isotherm study, the Stern-Volmer equations under different temperatures are shown in Fig. S5. Results showed that the Stern – Volmer quenching constant $K_{SV}$ was negatively correlated with temperature ($K_{SV}$ =1192 or 977 $M^{-1}$, at 293K or 298K, respectively), indicating that the probable quenching mechanism is static rather than dynamic quenching. This observation is consistent with

the speculation that $Cu^{2+}$ might interact with BTC ligand within MOF-76(Tb), resulting in static quenching.

## 4. Conclusion

In this work, the domestic silk fiber was utilized as the skeleton for the coating of luminescent MOF-76(Tb). Results show that the silk fiber could be a potential substrate candidate for MOFs coating. Comparing the three synthesis methods (HT, MWA, and LBL) used for MOF-76(Tb) coating, the LBL method could achieve a higher coating efficiency due to the enhanced metal ion anchoring process and the strictly controlled crystal growth. In addition, this new composite could be extended for utilization in colorimetric and fluorescent detection of $Cu^{2+}$ with a low detection limit of 0.5 mg/L. Being different from traditional powdered materials, the MOF-76-coated silk fiber can offer great application potential in real practice because of its convenient usage.

## Acknowledgements

This work was supported by the National Science Foundation of China (NSFC, No. 21777119 & 21577100), Science & Technology Commission of Shanghai Municipality (17230711600, 17DZ2200900), Shanghai Rising-Star Program (18QA1404300), the Fundamental Research Funds for the Central Universities (22120180102), and Young Excellent Talents in Tongji University (2015KJ001). Mr. Jie Li would like to thank the financial support, provided by the Chinese Scholarship Committee (CSC) scholarship (201606260184) for his PhD study abroad.

## Appendix A. Supplementary data

Supplementary data associated with this article can be found in the online version.

## Notes

The authors declare no competing financial interest.

## References

[1] H. Furukawa, K.E. Cordova, M. O'Keeffe, O.M. Yaghi, The chemistry and applications of metal-organic frameworks, Science 341 (2013) 974-987.

[2] L.E. Kreno, K. Leong, O.K. Farha, M. Allendorf, R.P. Van Duyne, J.T. Hupp, Metal-organic framework materials as chemical sensors, Chem. Rev. 112 (2012) 1105-1125.

[3] R. Ozer, J. Hinestroza, One-step growth of isoreticular luminescent metal–organic frameworks on cotton fibers, RSC Adv. 5 (2015) 15198-15204.

[4] M.D. Allendorf, C.A. Bauer, R.K. Bhakta, R.J. Houk, Luminescent metal-organic frameworks, Chem. Soc. Rev. 38 (2009) 1330-1352.

[5] Y. Cui, B. Chen, G. Qian, Lanthanide metal-organic frameworks for luminescent sensing and light-emitting applications, Coord. Chem. Rev. 273-274 (2014) 76-86.

[6] W. Zhang, J. Yu, Y. Cui, X. Rao, Y. Yang, G. Qian, Assembly and tunable luminescence of lanthanide-organic frameworks constructed from 4-(3,5-dicarboxyphenyl)pyridine-2,6-dicarboxylate ligand, J. Alloys Compd. 551 (2013) 616-620.

[7] J.J. Qian, L.G. Qiu, Y.M. Wang, Y.P. Yuan, A.J. Xie, Y.H. Shen, Fabrication of magnetically separable fluorescent terbium-based MOF nanospheres for highly selective trace-level detection of TNT, Dalton. Trans. 43 (2014) 3978-3983.

[8] A. Lan, K. Li, H. Wu, D.H. Olson, T.J. Emge, W. Ki, M. Hong, J. Li, A luminescent microporous metal-organic framework for the fast and reversible detection of high

explosives, Angew. Chem. Int. Ed. 48 (2009) 2334-2338.

[9] S. Khanjani, A. Morsali, Layer by layer growth of nano porous lead(ii) coordination polymer on natural silk fibers and its application in removal and recovery of iodide, Cryst. Eng. Comm. 14 (2012) 8137.

[10] N.L. Rosi, J. Kim, M. Eddaoudi, B. Chen, M. O'Keeffe, O.M. Yaghi, Rod packings and metal− organic frameworks constructed from rod-shaped secondary building units, J. Am. Chem. Soc. 127 (2005) 1504-1518.

[11] B. Chen, L. Wang, F. Zapata, G. Qian, E.B. Lobkovsky, A luminescent microporous metal− organic framework for the recognition and sensing of anions, J. Am. Chem. Soc. 130 (2008) 6718-6719.

[12] W. Yang, Z.Q. Bai, W.Q. Shi, L.Y. Yuan, T. Tian, Z.F. Chai, H. Wang, Z.M. Sun, MOF-76: from a luminescent probe to highly efficient U(VI) sorption material, Chem. Commun. (Camb) 49 (2013) 10415-10417.

[13] X. Lian, B. Yan, A lanthanide metal–organic framework (MOF-76) for adsorbing dyes and fluorescence detecting aromatic pollutants, RSC Adv. 6 (2016) 11570-11576.

[14] W. Yang, J. Feng, S. Song, H. Zhang, Microwave-assisted modular fabrication of nanoscale luminescent metal-organic framework for molecular sensing, ChemPhysChem 13 (2012) 2734-2738.

[15] Y. Xiao, L. Wang, Y. Cui, B. Chen, F. Zapata, G. Qian, Molecular sensing with lanthanide luminescence in a 3D porous metal-organic framework, J. Alloys Compd. 484 (2009) 601-604.

[16] W. Wang, Y. Li, M. Sun, C. Zhou, Y. Zhang, Y. Li, Q. Yang, Colorimetric and

fluorescent nanofibrous film as a chemosensor for $Hg^{2+}$ in aqueous solution prepared by electrospinning and host–guest interaction, Chem. Commun. 48 (2012) 6040-6042.

[17] W. Wang, X. Wang, Q. Yang, X. Fei, M. Sun, Y. Song, A reusable nanofibrous film chemosensor for highly selective and sensitive optical signaling of $Cu^{2+}$ in aqueous media, Chem. Commun. 49 (2013) 4833-4835.

[18] W. Wang, Q. Yang, L. Sun, H. Wang, C. Zhang, X. Fei, M. Sun, Y. Li, Preparation of fluorescent nanofibrous film as a sensing material and adsorbent for $Cu^{2+}$ in aqueous solution via copolymerization and electrospinning, J. Hazard. Mater. 194 (2011) 185-192.

[19] Y. Zhang, S. Yuan, G. Day, X. Wang, X. Yang, H.-C. Zhou, Luminescent sensors based on metal-organic frameworks, Coordin. Chem. Rev. 354 (2018) 28-45.

[20] D. Zacher, O. Shekhah, C. Wöll, R.A. Fischer, Thin films of metal–organic frameworks, Chem. Soc. Rev. 38 (2009) 1418-1429.

[21] R.M. Abdelhameed, O.M. Kamel, A. Amr, J. Rocha, A.M. Silva, Anti-mosquito activity of a titanium-organic framework supported on fabrics, ACS Appl. Mater. Interfaces 9 (2017) 22112 −22120.

[22] M.J. Neufeld, A. Lutzke, J.B. Tapia, M.M. Reynolds, Metal–Organic Framework/chitosan hybrid materials promote nitric oxide release from s-nitrosoglutathione in aqueous solution, ACS Appl. Mater. Interfaces 9 (2017) 5139-5148.

[23] M.J. Neufeld, B.R. Ware, A. Lutzke, S.R. Khetani, M.M. Reynolds, Water-stable Metal–Organic Framework/polymer composites compatible with human hepatocytes,

ACS Appl. Mater. Interfaces 8 (2016) 19343-19352.

[24] M. Meilikhov, K. Yusenko, E. Schollmeyer, C. Mayer, H.J. Buschmann, R.A. Fischer, Stepwise deposition of metal organic frameworks on flexible synthetic polymer surfaces, Dalton. Trans. 40 (2011) 4838-4841.

[25] P. Küsgens, S. Siegle, S. Kaskel, Crystal growth of the Metal—Organic Framework $Cu_3(BTC)_2$ on the surface of pulp fibers, Adv. Eng. Mater. 11 (2009) 93-95.

[26] X. Xiao, X. Liu, F. Chen, D. Fang, C. Zhang, L. Xia, W. Xu, Highly anti-UV properties of silk fiber with uniform and conformal nanoscale $TiO_2$ coatings via atomic layer deposition, ACS Appl. Mater. Interfaces 7 (2015) 21326-21333.

[27] J. Nam, Y.H. Park, Morphology of regenerated silk fibroin: Effects of freezing temperature, alcohol addition, and molecular weight, J. Appl. Polym. Sci. 81 (2001) 3008-3021.

[28] J. Pérez-Rigueiro, M. Elices, J. Llorca, C. Viney, Effect of degumming on the tensile properties of silkworm (Bombyx mori) silk fiber, J. Appl. Polym. Sci. 84 (2002) 1431-1437.

[29] A.R. Abbasi, K. Akhbari, A. Morsali, Dense coating of surface mounted CuBTC Metal-Organic Framework nanostructures on silk fibers, prepared by layer-by-layer method under ultrasound irradiation with antibacterial activity, Ultrason. Sonochem. 19 (2012) 846-852.

[30] A.R. Abbasi, J.a.-D. Aali, A. Azadbakht, A. Morsali, V. Safarifard, Synthesis and characterization of TMU-16-$NH_2$ metal-organic framework nanostructure upon silk fiber: study of structure effect on morphine and methyl orange adsorption affinity, Fiber.

Polym. 16 (2015) 1193-1200.

[31] O. Shekhah, H. Wang, S. Kowarik, F. Schreiber, M. Paulus, M. Tolan, C. Sternemann, F. Evers, D. Zacher, R.A. Fischer, Step-by-step route for the synthesis of metal− organic frameworks, J. Am. Chem. Soc. 129 (2007) 15118-15119.

[32] M.R. Awual, A novel facial composite adsorbent for enhanced copper(II) detection and removal from wastewater, Chem. Eng. J. 266 (2015) 368-375.

[33] M.R. Awual, T. Yaita, S.A. El-Safty, H. Shiwaku, S. Suzuki, Y. Okamoto, Copper(II) ions capturing from water using ligand modified a new type mesoporous adsorbent, Chem. Eng. J. 221 (2013) 322-330.

[34] J. Yao, K. Zhang, H. Zhu, F. Ma, M. Sun, H. Yu, J. Sun, S. Wang, Efficient ratiometric fluorescence probe based on dual-emission quantum dots hybrid for on-site determination of copper ions, Anal. Chem. 85 (2013) 6461-6468.

[35] C. Liu, B. Yan, A novel photofunctional hybrid material of pyrene functionalized metal-organic framework with conformation change for fluorescence sensing of $Cu^{2+}$, Sensor. Actuat. B-Chem. 235 (2016) 541-546.

[36] W. Lamoolphak, W. De-Eknamkul, A. Shotipruk, Hydrothermal production and characterization of protein and amino acids from silk waste, Bioresour. Technol. 99 (2008) 7678-7685.

[37] B. Mortimer, J. Guan, C. Holland, D. Porter, F. Vollrath, Linking naturally and unnaturally spun silks through the forced reeling of Bombyx mori, Acta Biomater. 11 (2015) 247-255.

[38] G. Wu, P. Song, D. Zhang, Z. Liu, L. Li, H. Huang, H. Zhao, N. Wang, Y. Zhu,

Robust composite silk fibers pulled out of silkworms directly fed with nanoparticles, Int. J. Biol. Macromol. 104 (2017) 533-538.

[39] N.L. Rosi, J. Kim, M. Eddaoudi, B. Chen, M. O'Keeffe, O.M. Yaghi, Rod packings and metal-organic frameworks constructed from rod-shaped secondary building units, J. Am. Chem. Soc. 127 (2005) 1504-1518.

[40] J. Zhao, B. Gong, W.T. Nunn, P.C. Lemaire, E.C. Stevens, F.I. Sidi, P.S. Williams, C.J. Oldham, H.J. Walls, S.D. Shepherd, M.A. Browe, G.W. Peterson, M.D. Losego, G.N. Parsons, Conformal and highly adsorptive metal–organic framework thin films via layer-by-layer growth on ALD-coated fiber mats, J. Mater. Chem. A 3 (2015) 1458-1464.

[41] Y. Xiao, L. Wang, Y. Cui, B. Chen, F. Zapata, G. Qian, Molecular sensing with lanthanide luminescence in a 3D porous metal-organic framework, J. Alloys Compd. 484 (2009) 601-604.

[42] C.-Z. Zhou, F. Confalonieri, N. Medina, Y. Zivanovic, C. Esnault, T. Yang, M. Jacquet, J. Janin, M. Duguet, R. Perasso, Fine organization of Bombyx mori fibroin heavy chain gene, Nucleic Acids Res. 28 (2000) 2413-2419.

[43] Y. Shen, M.A. Johnson, D.C. Martin, Microstructural characterization of Bombyx mori silk fibers, Macromol. 31 (1998) 8857-8864.

[44] M.J. Neufeld, J.L. Harding, M.M. Reynolds, Immobilization of Metal-Organic Framework Copper(II) benzene-1,3,5-tricarboxylate (CuBTC) onto cotton fabric as a nitric oxide release catalyst, ACS Appl. Mater. Interfaces 7 (2015) 26742-26750.

[45] M. Liu, G. Li, Z. Cheng, A novel dual-functional fluorescent chemosensor for the

selective detection of 2,4,6-trinitrotoluene and $Hg^{2+}$, New J. Chem. 39 (2015) 8484-8491.

[46] M. Almáši, V. Zeleňák, J. Kuchár, S. Bourrelly, P.L. Llewellyn, New members of MOF-76 family containing Ho(III) and Tm(III) ions: characterization, stability and gas adsorption properties, Colloid. Surface. A 496 (2016) 114-124.

[47] J. Ethiraj, F. Bonino, J.G. Vitillo, K.A. Lomachenko, C. Lamberti, H. Reinsch, K.P. Lillerud, S. Bordiga, Solvent-driven gate opening in MOF-76-Ce: effect on $CO_2$ adsorption, ChemSusChem 9 (2016) 713-719.

[48] A.R. Abbasi, K. Akhbari, A. Morsali, Dense coating of surface mounted CuBTC metal–organic framework nanostructures on silk fibers, prepared by layer-by-layer method under ultrasound irradiation with antibacterial activity, Ultrason. Sonochem. 19 (2012) 846-852.

[49] N.A. Khan, S.H. Jhung, Synthesis of metal-organic frameworks (MOFs) with microwave or ultrasound: Rapid reaction, phase-selectivity, and size reduction, Coordin. Chem. Rev. 285 (2015) 11-23.

[50] H. Guo, Y. Zhu, S. Qiu, J.A. Lercher, H. Zhang, Coordination modulation induced synthesis of nanoscale Eu(1-x)Tb(x)-metal-organic frameworks for luminescent thin films, Adv. Mater. 22 (2010) 4190-4192.

[51] T.-W. Duan, B. Yan, Hybrids based on lanthanide ions activated yttrium metal–organic frameworks: functional assembly, polymer film preparation and luminescence tuning, J. Mater. Chem. C 2 (2014) 5098-5104.

[52] W. Yang, J. Feng, H. Zhang, Facile and rapid fabrication of nanostructured

lanthanide coordination polymers as selective luminescent probes in aqueous solution, J. Mater. Chem. 22 (2012) 6819.

[53] J. Zhao, Y.N. Wang, W.W. Dong, Y.P. Wu, D.S. Li, Q.C. Zhang, A robust luminescent Tb(III)-MOF with Lewis basic pyridyl sites for the highly sensitive detection of metal ions and small molecules, Inorg. Chem. 55 (2016) 3265-3271.

[54] Z. Hao, X. Song, M. Zhu, X. Meng, S. Zhao, S. Su, W. Yang, S. Song, H. Zhang, One-dimensional channel-structured Eu-MOF for sensing small organic molecules and $Cu^{2+}$ ion, J. Mater. Chem. A 1 (2013) 11043.

[55] B. Liu, W.P. Wu, L. Hou, Y.Y. Wang, Four uncommon nanocage-based Ln-MOFs: highly selective luminescent sensing for $Cu^{2+}$ ions and selective $CO_2$ capture, Chem. Commun. (Camb) 50 (2014) 8731-8734.

**Supplementary Materials**

# From powder to cloth: facile fabrication of dense MOF-76(Tb) coating onto natural silk fiber for feasible detection of copper ions

Jie Li[a,b,d], Xiao Yuan[b,d], Yi-nan Wu[b,d,*], Xiaoliang Ma[b,d], Fengting Li[b,c,d], Bingru Zhang[b,c,d], Ying Wang[b,c,d,*], Zhongfang Lei[a,*], Zhenya Zhang[a]

[a] Graduate School of Life and Environmental Sciences, University of Tsukuba, 1-1-1 Tennodai, Tsukuba, Ibaraki 305-8572, Japan

[b] College of Environmental Science & Engineering, State Key Laboratory of Pollution Control and Resource Reuse Study, Tongji University, 1239 Siping Road, Shanghai 200092, China

[c] UNEP-Tongji Institute of Environment for Sustainable Development, Tongji University, Shanghai 200092, China

[d] Shanghai Institute of Pollution Control and Ecological Security, Shanghai 200092, China

*Corresponding authors.

Email addresses: 51n@tongji.edu.cn (Y. Wu), yingwang@tongji.edu.cn (Y. Wang), lei.zhongfang.gu@u.tsukuba.ac.jp (Z. Lei)

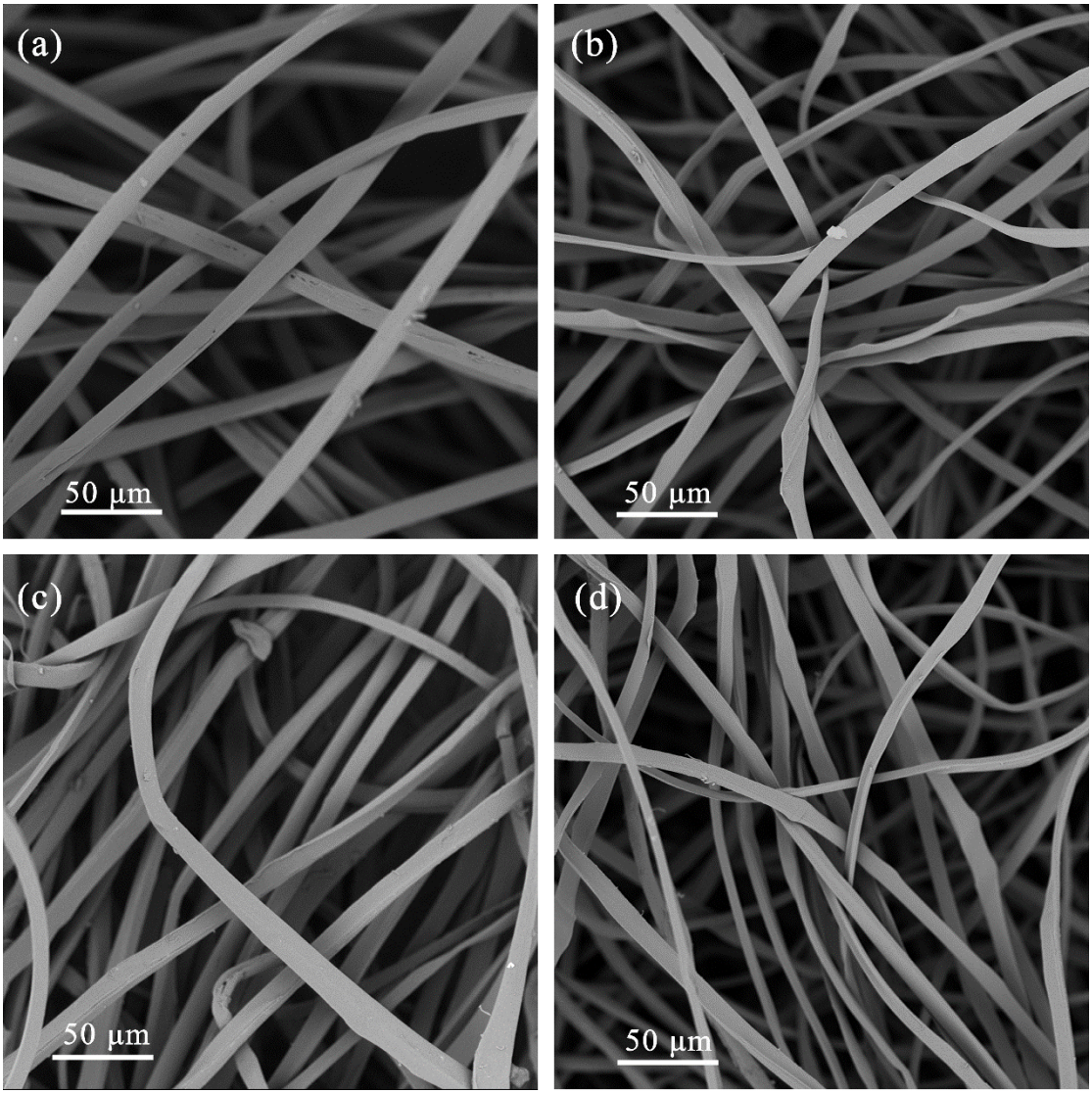


Fig. S1 SEM images of domestic silk fiber after immersion in various solvents at 80 ˚C for 24 h: (a) water; (b) DMF; (c) ethanol; and (d) n-hexane;

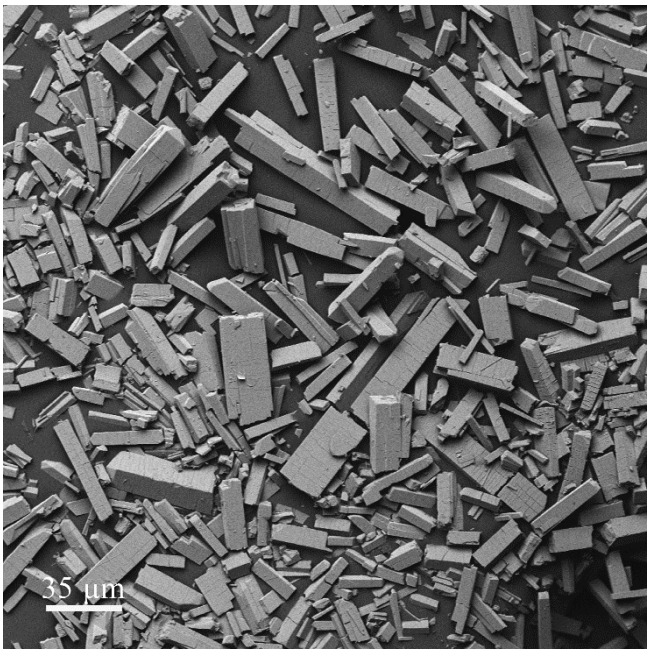


Fig. S2 SEM image of the MOF-76(Tb) material synthesized with hydrothermal method.

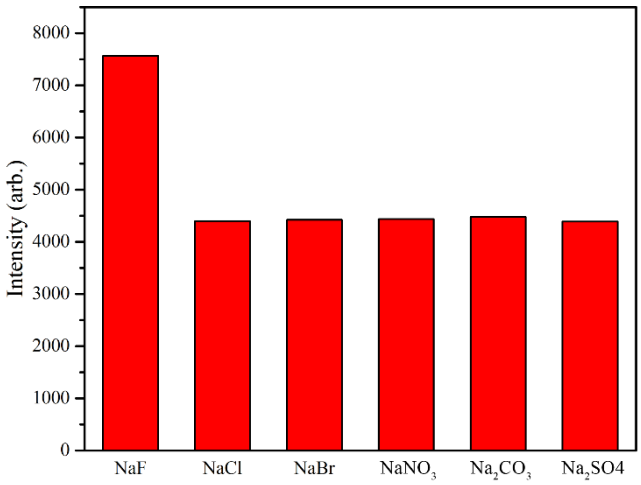


Fig. S3 Luminescence intensity of the MOF-76(Tb)@silk fiber in 0.5 mM of various anion containing solutions (at 548 nm)

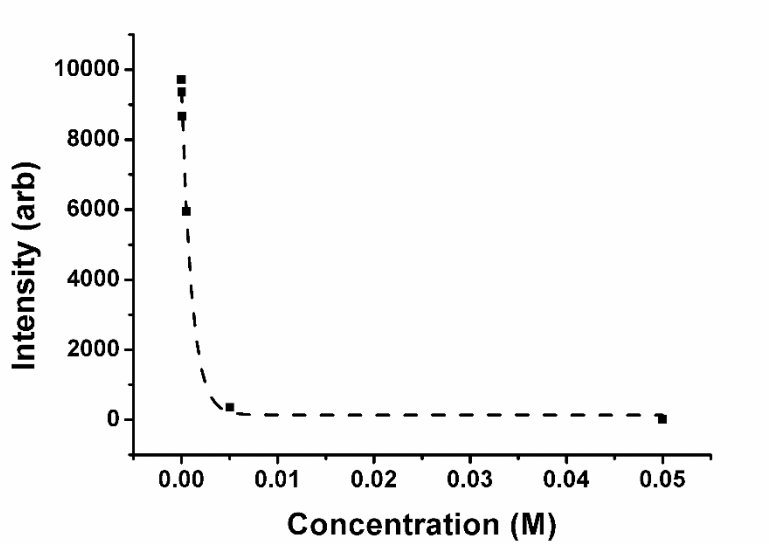


Fig. S4 Decrease of the luminescence intensity at 548 nm along with the concentration of $Cu^{2+}$. The dashed line represents an exponential equation fit to the data.

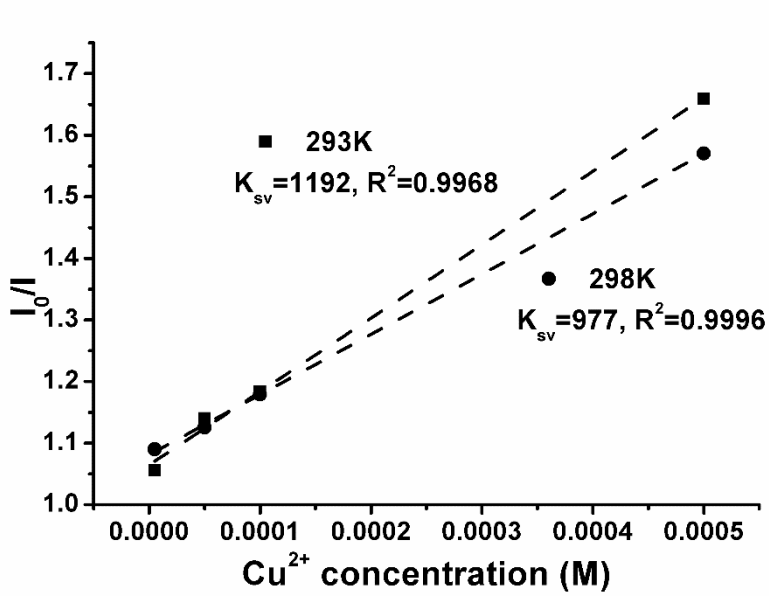


Fig. S5 Stern–Volmer plots of silk fibroin composite for sensing $Cu^{2+}$ in the range of $10^{-3}$–$10^{-5}$ M at different temperatures. The dashed line represents a linear fit to the data.